DISCUSSION ON THE EFFECTS OF STRUCTURAL PARAMETERS OF ROUGHNESS ON HEAT TRANSFER SIMILARITY

Rika Nagura[1], Wataru Yagasaki[1], Yusuke Kuwata[1*], Kazuhiko Suga[1]

[1]Department of Mechanical Engineering, Osaka Prefecture University, Sakai, Osaka 599-8531, Japan

1. INTRODUCTION

We see rough walls everywhere in the real world. Scientists and engineers have been thus dedicating to elucidating the rough-wall flow physics to avoid or utilize the effects of surface roughness. The wall roughness increases friction drag, leading to a downward shift in the logarithmic mean velocity. It is well established that the downward shift value, which is referred to as the velocity roughness function ΔU^+, can be scaled by the equivalent sand grain roughness height k_s^+[1], and the current remaining issue is how to estimate k_s^+ from the topological parameters of rough surfaces [2]. As for heat transfer, many numerical and experimental studies reported that wall roughness leads to the breakdown of the similarity between the momentum and heat transfer [3,4]; however, comparatively little attention has been paid to the scaling of the heat transfer over rough surfaces. The experimental studies by Dipprey & Sabersky [5] and Kays & Crawford [6] proposed a correlation for the Stanton number over rough surfaces, which can be rewritten in terms of the velocity roughness function ΔU^+ and temperature roughness function $\Delta\Theta^+$[7]:

$$\Delta\Theta^+ = \Delta U^+ - A{k_s^+}^{0.2} Pr^{0.44} + B - \beta(Pr) \tag{1}$$

with $A = 5.19, B = -3.3$ and $\beta(0.71) = 3.0$ [5] for a surface with sand-grain roughness, while Kays-Crawford [6] suggested $A = 1.25$ and $B = 5.2$ from the data for packed-spheres. That is, the coefficients of these two studies are significantly different. The recent direct numerical simulation (DNS) data by McDonald et al. [3] over sinusoidal-roughness elements reasonably agreed with Dipprey & Sabersky's (D-S) correlation, while Bons [8] concluded that D-S correlation yielded a better prediction for realistic rough surfaces. It is hence reasonable to conjecture that some topological parameters for rough surfaces determine those coefficients. Although there are many relevant parameters that may affect the scaling of $\Delta\Theta^+$, this study focuses on the effects of a wavelength of surface undulations on the turbulent heat transfer. To this end, we carried out DNSs for sinusoidal rough surfaces with different wavelengths by the lattice Boltzmann method (LBM). We discuss the effects of the wavelengths on the temperature roughness function and Reynolds analogy, and provide information on the underlying physical mechanism for rough wall turbulent heat transfer.

2. DNS SCHEME AND FLOW CONDITIONS

The double distribution-function LBM was applied to calculate turbulent forced-convection heat transfer in open channel flows over rough surfaces. This LBM consists of the D3Q27 multiple-relaxation-time model and the D3Q19 regularized lattice BGK model for the flow and thermal fields, respectively. This scheme is stable and accurate for simulating turbulent heat transfer in complex geometries as demonstrated in many different flow fields such as Ref. [9]. A schematic of a rough-walled open-channel flow is shown in Figure 1. The bottom wall was a three-dimensional sinusoidal rough surface while the slip boundary conditions were applied to the top boundary face. The flow was periodic in the streamwise (x) and spanwise (z) directions, and it was driven by a streamwise constant pressure difference. The friction Reynolds number based on the effective half channel height δ_e and the averaged friction velocity u_τ was varied: $Re_\tau = 180$, 300, and 600, where $\delta_e = \delta - k$ stands for the distance from the mean roughness height to the top boundary. The computational domain was $6\delta_e(x) \times \delta_e(y) \times 3\delta_e(z)$ in the streamwise, wall-normal, and spanwise directions. The incompressible fluid with a uniform internal heat generation was considered, and the fluid Prandtl number Pr was 0.7 assuming

*Corresponding Author: kuwata@me.osakafu-u.ac.jp

an air flow. A constant wall temperature T_w was imposed for the rough surfaces, while the top boundary was adiabatic. In the following, we consider the temperature variance $\theta = T - T_w$ with T being the fluid temperature.

The rough surface under consideration is a three-dimensional sinusoidal rough surface where the height of the rough surface $h(x,z)$ was given as follows [3]:

$$h(x,z) = k\left(1 + \cos\left(\frac{2\pi x}{\lambda_x}\right)\cos\left(\frac{2\pi z}{\lambda_z}\right)\right), \quad (1)$$

where k is the surface amplitude, λ_x and λ_z are the streamwise and spanwise wavelengths of undulations, respectively. We considered a fixed surface amplitude $k = \delta/11.5$ while varying the wavelengths of $\lambda_x = \lambda_z = \lambda = 2k, 4k, 8k$ and $16k$. We also performed three reference smooth-wall simulations at $Re_\tau = 180$, 300, and 600. We considered uniform spacing of grids and determined the grid resolution, adhering to the guideline that the resolution in wall units is less than 2.0 [7,11]. The resultant grid points were $640(x) \times 116(y) \times 320(z)$ at $Re_\tau = 180$, $896(x) \times 162(y) \times 448(z)$ at $Re_\tau = 300$, and $1536(x) \times 278(y) \times 767(z)$ at $Re_\tau = 600$. The rough surfaces were resolved by 19, 27 and 47 grids in the vertical direction at $Re_\tau = 180, 300$, and 600, respectively.

As the local wall shear stress and wall heat flux at the rough surfaces have considerable spatial variations, we considered the average wall shear stress and wall heat flux. The average friction velocity u_τ was computed from the wall shear stress τ_w as $u_\tau = \sqrt{\tau_w/\rho}$, which is given from the momentum balance between the pressure difference in the streamwise direction ΔP and the equivalent wall shear stress τ_w as follows:

$$\tau_w L_x L_z = L_z(\delta - k)\Delta P. \quad (2)$$

The friction temperature was defined as $\theta_\tau = q_w/(\rho c u_\tau)$, where ρ is the fluid density, c is the specific heat, and q_w is the wall heat flux. Here, q_w was given from the energy balance between the amount of the heat generation in the domain and the wall heat flux offered by a reference plane, which is written as follows:

$$q_w L_x L_z = V_f S_{UHG}, \quad (3)$$

where S_{UHG} is the internal heat generation, and the total volume of the fluid is $V_f = \delta_e L_x L_z$.

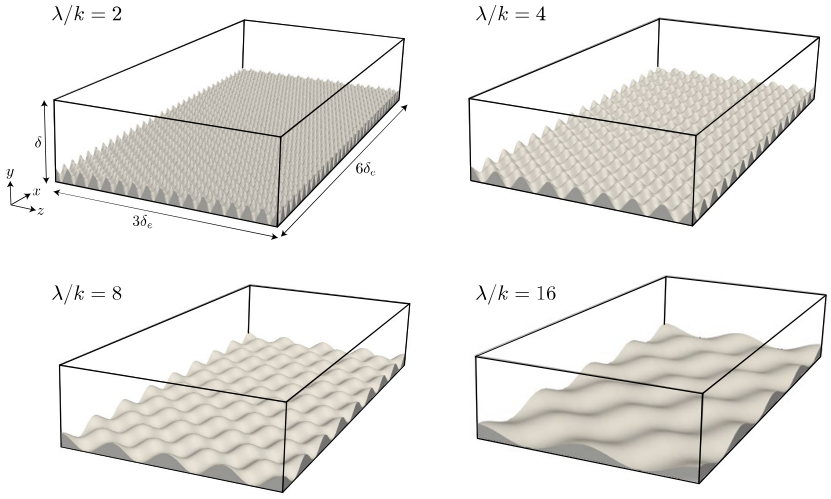

Figure 1 : Flow geometry of open channel flows over sinusoidal rough surfaces.

3. RESULTS AND DISCUSSION

Figure 2 compares inner-scaled mean velocity U^+ and temperature Θ^+ profiles at $Re_\tau = 180$ and 600. Below the roughness crest, the superficially x − z plane-averaged values are shown. The distance from rough surfaces is defined with the virtual origin, which is given as the zero-plane displacement, d, introduced by Jackson [12] :

$$d = \int_0^{2k} f_x y dy \Big/ \int_0^{2k} f_x dy, \tag{4}$$

where f_x is a sum of the mean viscous and pressure drag offered by the rough surface. Since $d > 0$, the origin of the vertical coordinate is shifted upward from the bottom of the rough surface. The figure confirms that the profiles of U^+ and Θ^+ for rough wall cases are considerably lower than the smooth wall profiles, which is due to the augmented momentum and heat transfer by wall roughness. In the logarithmic region, the profiles of U^+ and Θ^+ are shifted downward from the smooth wall profiles, while the slopes in the logarithmic region are almost unchanged. We can observe that the downward shift values of U^+ and Θ^+ in the logarithmic region, which are respectively referred to as the velocity roughness function ΔU^+ and temperature roughness function $\Delta\Theta^+$, increase with increasing Re_τ. Another observation is that the modifications of the U^+ and Θ^+ profiles depend on the wavelength λ/k value, and the λ/k value appears to affect $\Delta\Theta^+$ more than ΔU^+.

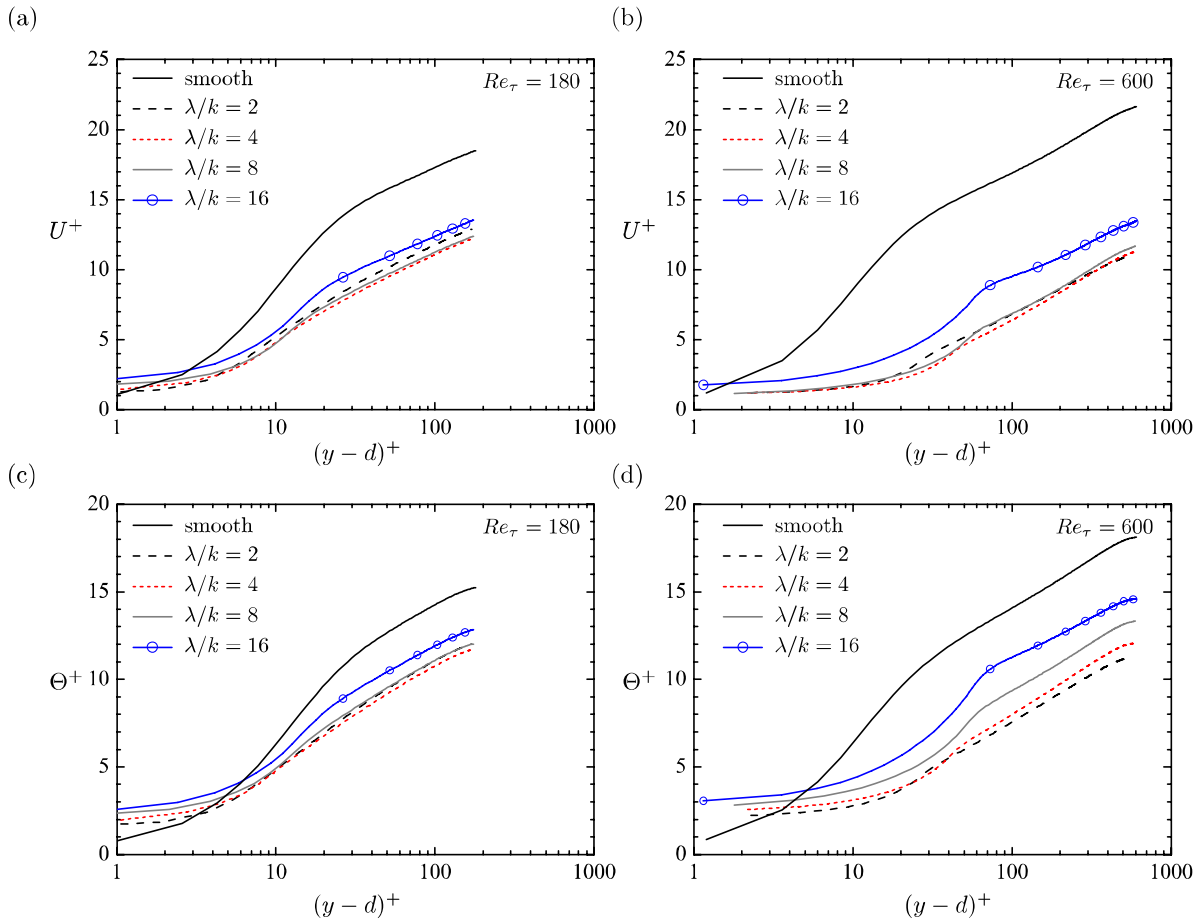

Figure 2 : Inner-scaled mean profiles with a semi-logarithmic format: (a) U^+ at $Re_\tau = 180$, (b) Θ^+ at $Re_\tau = 180$, (c) U^+ at $Re_\tau = 600$, and (d) Θ^+ at $Re_\tau = 600$.

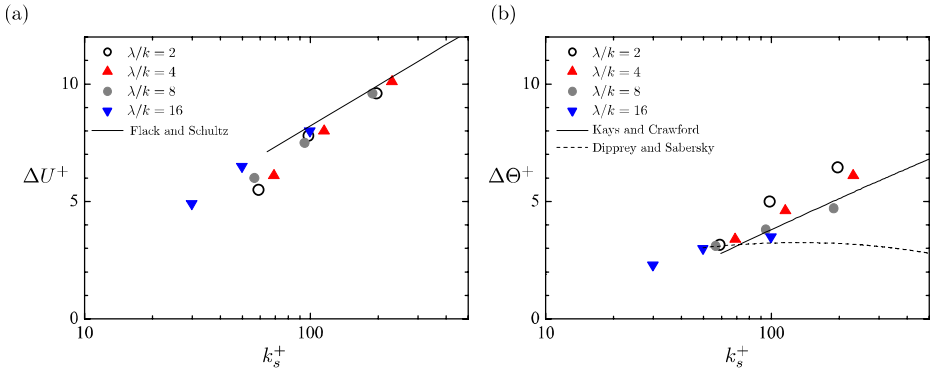

Figure 3 : (a) velocity roughness function ΔU^+, (b) temperature roughness function $\Delta\Theta^+$. The correlation for ΔU^+ in the fully rough regime[2], and the correlations by Kays and Crawford[5] and Dipprey and Sabersky[6] are included.

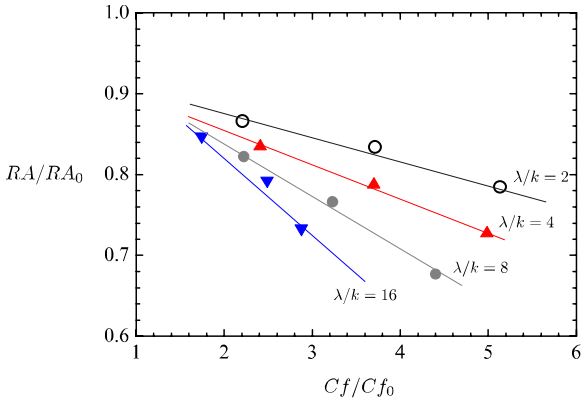

Figure 4 : Reynolds analogy factor RA/RA_0 against the skin friction increase ratio C_f/C_{f0}.

To examine the dependence of $\Delta U^+$and $\Delta\Theta^+$on Re_τ and λ/k in more detail, Figure 3 plots ΔU^+ and $\Delta\Theta^+$ against the inner-scaled equivalent roughness k_s^+. In Fig.3(a), ΔU^+ in the fully rough regime ($k_s^+ > 70$) follows the correlation [1] irrespective of the λ/k value, whereas the effect of the λ/k value is still visible in the asymptotic behaviour toward the fully rough regime. As for the temperature roughness function $\Delta\Theta^+$ in Fig.3(b), $\Delta\Theta^+$ near the onset of the fully rough regime at $k_s^+ \simeq 70$ takes an almost same value $\Delta\Theta^+ \simeq 3$ irrespective of the λ/k value, whereas in the fully rough regime, the λ/k value has a noticeable effect on $\Delta\Theta^+$. It is observed that $\Delta\Theta^+$ for long wavelength case of $\lambda/k = 16$ tends to be smaller, and close to the D-S correlation by Dipprey and Sabersky [5]. As the λ/k value decreases, $\Delta\Theta^+$ in the fully rough regime tends to increase, and $\Delta\Theta^+$ for short wavelength cases of $\lambda/k = 2$ and 4 are slightly above the K-S correlation by Kays and Crawford [6].

To discuss the similarity between the heat and momentum transfer, we discuss the Reynolds analogy factor RA. The RA value is defined as a ratio of the doubled Stanton number to the skin friction coefficient $RA = 2St/C_f$, and quantifies the similarity between the momentum and heat transfer. Figure 4 presents the RA values normalized by the corresponding smooth wall values RA_0 as a function of the skin friction increase ratio C_f/C_{f0} with C_{f0} being the skin friction coefficient for smooth wall. The figure shows that RA/RA_0 for rough wall cases is below unity, indicating the occurrence of the unfavourable dissimilarity. In other words, the wall roughness increases C_f more than St. The important finding from the figure is that RA/RA_0 decreases with increasing C_f/C_{f0}, and an increase in the λ/k value results in a steeper decrease in the RA/RA_0 value. This means that the breakdown of the Reynolds analogy is accompanied by an increase in C_f, and the wavy surface (i.e., the surface with larger λ/k value), yields stronger unfavourable dissimilarity between the momentum and heat transfer.

To understand underlying physical mechanisms of the unfavourable dissimilarity, we analyse the budget terms in the spatial (x − z plane) and time averaged momentum and energy equations. Applying the spatial and time (double) averaging operators to the momentum equation, we can obtain the double averaged momentum equation in non-dimensional form as follows [11]:

$$1-\frac{y_e}{\delta_e}=\frac{\partial\langle\bar{u}\rangle^+}{\partial y^+}-\langle\overline{u'v'}\rangle^+-\langle\tilde{\bar{u}}\tilde{\bar{v}}\rangle^+ +\int_{y^+}^{\delta^+} f_x^+\,dy^+, \tag{5}$$

where the effective wall-normal distance is $y_e=\int_0^y \varphi dy$ with φ being the porosity (fluid occupation ratio) in a x − z plane. The overbar $\bar{\phi}$ denotes the time-averaging of a variable ϕ, and ϕ' is its fluctuation value. The bracket $\langle\phi\rangle$ denotes the plane-averaging, and the dispersion is defined as $\tilde{\phi}=\phi-\langle\phi\rangle$. The second moments $\langle\overline{u'v'}\rangle$ and $\langle\tilde{\bar{u}}\tilde{\bar{v}}\rangle$ represent the Reynolds stress and dispersive covariance, respectively. In a similar fashion, we can obtain the double averaged energy equation as follows:

$$1-\frac{y_e}{\delta_e}=\frac{1}{P_r}\frac{\partial\langle\bar{\theta}\rangle^+}{\partial y^+}-\langle\overline{\theta'v'}\rangle^+-\langle\tilde{\bar{\theta}}\tilde{\bar{v}}\rangle^+ +\int_{y^+}^{\delta^+} s_w^+\,dy^+, \tag{6}$$

where $\langle\overline{\theta'v'}\rangle$ and $\langle\tilde{\bar{\theta}}\tilde{\bar{v}}\rangle$ represent the turbulent and dispersion heat fluxes, respectively. The integrand s_w is the wall heat transfer term, which represents the x − z plane-averaged wall heat flux offered by the rough surface. Subtraction of Eq.(6) from Eq.(5) yields

$$\frac{\partial}{\partial y^+}\left(\frac{\langle\bar{\theta}\rangle^+}{P_r}-\langle\bar{u}\rangle^+\right)=\underbrace{\left(-\langle\overline{u'v'}\rangle^+-\langle\tilde{\bar{u}}\tilde{\bar{v}}\rangle^+ +\langle\overline{\theta'v'}\rangle^+ +\langle\tilde{\bar{\theta}}\tilde{\bar{v}}\rangle^+\right)}_{SM}+\underbrace{\int_{y^+}^{\delta^+}(f_x^+-s_w^+)\,dy^+}_{WI}. \tag{7}$$

The terms in the right-hand side of Eq.(7) are grouped as the second moment contribution, SM, and the wall-interaction contribution WI, both of which represent the contributions to a difference between U^+ and Θ^+. The positive value of SM or WI increases the unfavourable dissimilarity; that is, the positive contribution increases C_f more than St, whereas the negative value leads an opposite effect. Figure 5 shows the terms SM and WI. The figure confirms that SM and WI have appreciable values within the rough surfaces, suggesting that the dissimilarity is dominantly due to the flow modifications within the rough surface. For the long wavelength cases with $\lambda/k=8$ and 16, the positive contribution is dominated by SM just above the mean height location at $y=k$. Hence, the reason for the significant dissimilarity for the long wavelength cases is that the momentum fluxes due to the combined effects of turbulence and dispersion outweigh the corresponding heat fluxes.

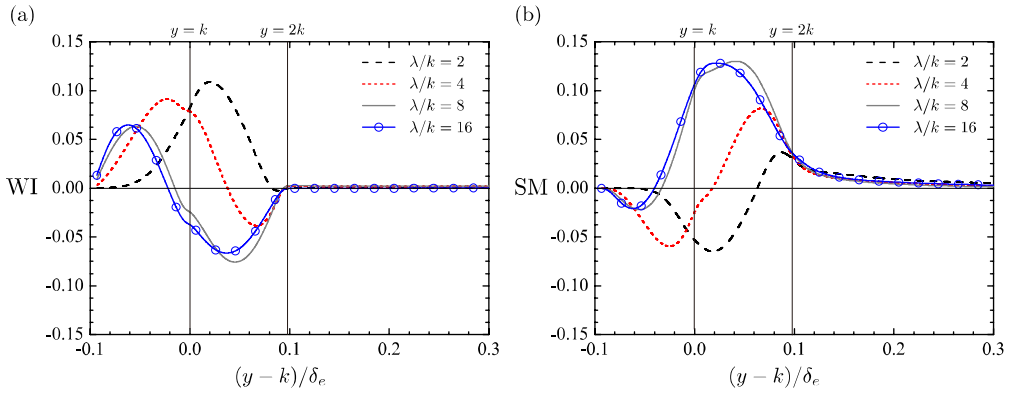

Figure 5 : Comparison of the contributors to the dissimilarity between the momentum and heat transfer: (a) second momentum contribution SM and (b) wall-interaction contribution WI.

4. CONCLUSIONS

Direct numerical simulations of turbulent heat transfer over three-dimensional sinusoidal rough surfaces were performed to discuss the scaling of the turbulent heat transfer over rough surfaces. The particular attention of this study was paid to the effect of a wavelength of surface undulations on the turbulent heat transfer. The wall roughness leads to the unfavourable breakdown of the analogy between the heat and momentum transfer; that is, the wall roughness increases the momentum transfer more than the heat transfer. It is confirmed that this unfavourable dissimilarity is more significant for the wavy rough surfaces with a long wavelength. The correlation by Dipprey and Sabersky [5] reasonably predicts the temperature roughness function for the surfaces with a longer wavelength, whereas the correlation by Kays and Crawford [6] gives better prediction for the surfaces with a short wavelength. To obtain physical understanding of the mechanisms of the dissimilarity between the heat and momentum transfer, we analysed the momentum and energy budgets. This analysis shows that the strong dissimilarity for the wavy surfaces with a long wavelength is due to a significantly increased momentum fluxes by the Reynolds stress and dispersive covariance. The momentum flux due to the combined effects of turbulence and dispersion outweigh the corresponding heat flux, resulting an increase in the skin friction coefficient more than the Stanton number.

REFERENCES

[1] J. Nikuradse, Laws of flow in rough pipes, VDI Forschungsheft, (1933).

[2] K. A. Flack & M. P. Schultz, Roughness effects on wall-bounded turbulent flows. *Phys. Fluids*, **26** (2014) 1013051.

[3] M. MacDonald, N. Hutchins & D. Chung, Roughness effects in turbulent forced convection. *J. Fluid Mech*., **861** (2019) 138-162.

[4] J.W.R. Peeters & N.D. Sandham, Turbulent heat transfer in channels with irregular roughness. *Int. J. Heat Mass Transf.,* **138** (2019) 454-467.

[5] D. F. Dipprey & R. H. Saberksy, Heat and momentum transfer in smooth and rough tubes at various Prandtl numbers. *Int. J. Heat Mass Transf*., **5** (1963) 329-353.

[6] W. M. Kays & M. Crawford, *Convective Heat and Mass Transfer*, McGraw-Hill, (1993).

[7] Y. Kuwata, Direct numerical simulation of turbulent heat transfer on the Reynolds analogy over irregular rough surfaces. *Int. J. Heat Fluid Flow*, **92** (2021) 108859.

[8] J.P. Bons, St and Cf augmentation for real turbine roughness with elevated freestream turbulence. *ASME Turbo Expo 2002: Power for Land, Sea, and Air,* (2002) 349-363.

[8] K. Suga, R. Chikasue & Y. Kuwata, Modelling turbulent and dispersion heat fluxes in turbulent porous medium flows using the resolved LES data. *Int. J. Heat Fluid Flow*, **68** (2017) 225–236.

[11] Y.Kuwata & Y. Kawaguchi, Direct numerical simulation of turbulence over systematically varied irregular rough surfaces. *J. Fluid Mech*., **862**(2019) 781-815.

[12] P.S. Jackson, On the displacement height in the logarithmic velocity profile. *J. Fluid Mech*., **111** (1981) 15-25.